

Length scales in crystal plasticity

K. Sieradzki *, A. Rinaldi, C. Friesen, P. Peralta

Fulton School of Engineering, Arizona State University, Tempe, AZ 85287-6106, USA

Received 20 April 2006; received in revised form 22 May 2006; accepted 22 May 2006

Available online 22 August 2006

Abstract

Significant effects of sample dimension on the yield strength of metallic crystals have been known for more than 50 years when researchers identified this phenomenon in metallic whiskers. These sample-size effects are once again attracting great interest with the discovery of the indentation size effect and the enhanced yield strength found for sub-micrometer diameter focused ion beam (FIB)-machined metallic pillars. Here, we discuss these issues and suggest mechanisms that may be responsible for the observed behaviors. In the case of FIB-machined pillars we draw an analogy between the yield strength of these structures and the fracture strength of glass rods and suggest that the experimentally observed yield behavior in these pillars is consistent with that expected from extreme value statistics. Additionally, we revisit the topic of surface effects in crystal plasticity and suggest a new mechanism via which a free surface could act as a measurable source of hardening for a crystal that has a bulk interior free of defects such as dislocations or grain boundaries. Finally we suggest experimental approaches that can be used to test the ideas discussed herein.

© 2006 Published by Elsevier Ltd on behalf of Acta Materialia Inc.

Keywords: Yield strength; Crystal plasticity; Extreme value statistics

1. Introduction

The mechanical properties of nanoscale structures (less than $\sim 1 \mu\text{m}$) such as metallic whiskers have been studied for more than 50 years [1]. More recently, compression testing of focused ion beam (FIB)-machined nanopillars has demonstrated that plastic properties such as yield strength in these dimensionally constrained structures can approach the theoretical shear strength [2–6]. In many ways the results of the modern work are similar to those obtained for whiskers: at size scales of the order of $1 \mu\text{m}$ and below, there is a rapid rise in strength of the structure with decreasing diameter. Currently our understanding of these effects is incomplete but it seems that as surface to volume ratios increase there is a fundamental change in the physics controlling mechanical behavior. Herein, we discuss these length-scale effects and introduce some con-

cepts that may prove useful in understanding these phenomena.

Consider the load–displacement behavior of a dislocation-free gold single crystal rod. The lateral surfaces of the rod have the equilibrium structure defined by the Wulff construction. The initial load–displacement behavior will be linear elastic and will remain so until the stresses are high enough to either nucleate dislocations or cause the rod to fracture. Since gold is an intrinsically ductile material, we expect dislocation nucleation will occur prior to the conditions required for fracture of the rod. Dislocations can in principle either nucleate homogeneously within the rod interior or heterogeneously at the free surface of the rod. Years ago, Hirth [7] and Nabarro [8] considered this sort of scenario and concluded that nucleation at the free surface would occur prior to homogenous nucleation within the bulk of the solid. It is likely that surface defects would act as stress concentrators for nucleation. These defects could be surface steps (e.g. a vicinal surface) or corners (associated with the Wulff construction) or subtle scratches on the lateral surface of the

* Corresponding author.

E-mail address: Karl.Sieradzki@asu.edu (K. Sieradzki).

crystal. The magnitude of the shear stress required for the nucleation process would in general be expected to be quite large, i.e., of the order of the theoretical shear stress, since the stress concentration associated with steps or corners is of order 2. (The stress concentration for a scratch-like defect may be more severe.) Once a dislocation is nucleated from the surface we can expect that the dislocation will travel through the otherwise perfect crystal and presumably exit at the opposite end. The remnant of this process will be a surface step at the nucleation site and a surface step at the exit point. In fact, depending on the configuration of the dislocation, the step could circumscribe the entire crystal surface. In a stiff apparatus under load control (e.g., a weight hanging from the rod), the load–displacement behavior will adopt zero-slope over a displacement excursion corresponding to the magnitude of the dislocation Burgers vector. Following the initial nucleation event we can expect continued events to occur at fixed load (perfectly plastic behavior) until or unless the source configuration changes. A geometric change in the source configuration could make it more difficult (e.g., blunting of a scratch) or less difficult (stress concentration due to remnant steps from prior nucleation events) for continued nucleation. This could lead to a mild form of hardening or softening in the load–displacement curve.

The scenario that we have just described has been observed by Nix and co-workers in a series of publications [2–4] and more recently by Volkert and Lilleodden [5,6]. Using FIB techniques for making gold pillars they examined the load–displacement behavior in compression as a function of pillar diameter. They reported flow stresses of 550 MPa for 400 nm diameter single-crystal gold pillars, and load–displacement curves with the generic features outlined above. For electrodeposited cylinders they reported 1 GPa flow stresses for 1000 nm diameter cylinders; however, cross-sectional microscopy of these structures revealed that these pillars were polycrystalline.

Interestingly enough, our discussion in the previous paragraph was completely uncoupled to sample-size effects. Thus, it is probable that these sample size effects simply result from the likelihood of obtaining more perfect (fewer dislocations) crystals as crystal volumes are decreased. This is reminiscent of statistical concepts in brittle fracture and correspondingly well-known sample-size effects. Here for example extreme value statistics argues that the fracture stress should scale as a power law, in L or $\ln L$, where L is a measure of the sample size [9,10]. We wonder whether or not similar statistical approaches are appropriate for understanding sample-size effects in plasticity.

Consider, now the load–displacement behavior of a single-crystal gold rod containing a single axial screw dislocation. Also, suppose that there is an excess of vacancies in the volume of the rod that will tend to condense into prismatic loops in the vicinity of the dislocation causing it to adopt a helical form along some portion of the length of the rod [11,12]. Once again, we will suppose that the lateral surfaces of the rod have the equilibrium structure defined

by the Wulff construction. The initial load–displacement behavior will be linear elastic and will remain so until the nucleation of mobile dislocations. Fig. 1 illustrates how the nucleation of a glide dislocation from a surface source can result in the formation of a Frank–Read source at locations where the helix intersects the slip plane. Different scenarios may involve surface nucleation of a glide dislocation that intersects with a pair of oppositely signed screw dislocations or an axial helical dislocation of mixed character. In any event, a high stress level of the order of the theoretical shear strength may be required for the operation of the surface source but owing to the subsequent development of a dislocation mill continued dislocation nucleation could occur at significantly reduced stress levels. Once a dislocation is nucleated we can expect that the dislocation will travel through the otherwise perfect crystal and presumably exit at the opposite end leaving a remnant step at the exit point. Following the initial nucleation event, continued events may occur at reduced load until the source configuration changes. For the case considered above, continued nucleation from the Frank–Read source could result in unwinding of the helix (a process that may involve double-cross-slip) configuring other like sources on nearby parallel slip planes resulting in bands of deformation (i.e., Lüders bands) that propagate along the sample length. In a displacement-controlled test, the load–displacement curve will remain linear elastic to a high stress level (corresponding to that required for source configuration) and undergo a sharp yield with a load drop as dislocations are emitted from the now active source(s). Perfectly plastic behavior at the lower yield point will ensue with fluctuations in the load–displacement curve corre-

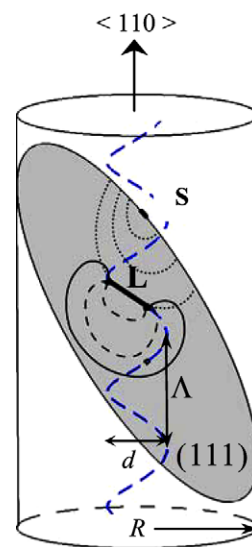


Fig. 1. A portion of a fcc whisker of radius R ($\sim 1 \mu\text{m}$) containing an axial helical screw dislocation of pitch Λ and radius $d/2$ such that $\Lambda \sim d \sim 100 \text{ nm}$. In general the helix can intersect the slip plane in three locations separated by a distance L of the order of 100 nm. A glide dislocation emitted from a surface source S , impinges on two points of the helix intersecting the slip plane resulting in the formation of a Frank–Read source. Once configured, this dislocation mill operates at a considerably reduced stress compared to that required for surface nucleation.

sponding to activation of sources on parallel planes and propagation of Lüders bands.

The load–displacement behavior that we have just described has been observed for “single crystal” metal whiskers as discussed by researchers such as Brenner 50 years ago [13]. The differentiation between this behavior and that described for the FIB-machined pillars may simply be the nature of the operative dislocation sources. In each of these cases the metal sample is perfect or nearly so in terms of dislocation content. Sample size via extreme value statistics controls the likelihood of a surface dislocation source operating which determines the stress level of the initial yield event(s). However, in the case of the whisker the presence of an axial dislocation may allow for the development of a dislocation mill which would result in a considerably reduced flow stress.

Now consider the effect of imposing a dilute oriented microstructure such as a single grain boundary running parallel to the axis of the gold rod. Assume no dislocation sources present in the interior of the rod so that we have a scenario relating to the operation of a surface source. The situation will evolve as described earlier except that now the boundary will act as an impediment to dislocation motion resulting in hardening. Thus we naturally expect that the flow stress will be larger than that observed for the perfect defect-free single crystal and that the grain size (in the case of a bi-crystal) imposes a microstructural length scale that serves as a barrier to dislocation motion. Note that here we are not describing the situation in a conventional polycrystalline material which contains many grown in dislocation sources that will be operative at low stress levels compared to that required for the operation of a surface source. In this scenario, owing to statistical issues, sample size sets the degree of perfection (dislocation and source content) in the material and the microstructural length scale determines flow behavior.

Finally consider a gold “rod” of diameter D with an oriented composite “microstructure” composed of parallel arrays of smaller diameter rods d (i.e., an one-dimensional parallel bar assembly as shown schematically in Fig. 2) such that $nd < D$, where n is the number of such rods in the width D . Each of the smaller rods is a “perfect” crystal in itself but there is a statistical distribution in the yield strength of the individual rods owing to fluctuations in

the nature of surface defects. We assume that the yield strength dependence on the rod diameter follows a power law, $\sigma_{\text{yield}} \sim d^{-\beta}$ ($\beta > 0$), as would be expected for a system obeying extreme value statistics of a Weibull form. Since the degree of perfection in the rod increases with decreasing diameter d , under what conditions will the yield strength of this parallel bar array exceed that of a homogeneous perfect crystal of diameter D ? It is convenient to employ a Gibson–Ashby relation for the effective Young’s modulus, E^* , for the parallel bar array:

$$(E^*/E) = C(\rho^*/\rho)^2 \quad (1)$$

where E is Young’s modulus of the homogeneous material (i.e., the solid bar of diameter D), ρ^* and ρ correspond to the density of the parallel bar solid and the homogeneous material and C is a constant very nearly equal to 1 [14]. In this one-dimensional parallel bar model $\rho^*/\rho = nd/D$ (in two dimensions $\rho^*/\rho = nd^2/D^2$). The stress–strain behavior is taken to be linear elastic up to the initial yield event for both the parallel bar solid and the cylinder of diameter D and is described by

$$\sigma_{\text{PB}} = E^* \varepsilon_{\text{PB}} = E(\rho^*/\rho)^2 \varepsilon_{\text{PB}} \quad (2a)$$

and

$$\sigma_D = E \varepsilon_D \quad (2b)$$

where the subscripts refer to the constitutive relations for the parallel bar assembly and homogeneous bar of diameter D . The Weibull behavior of these systems requires that at yield, $\varepsilon_{\text{PB}} \sim d^{-\beta}$ and $\varepsilon_D \sim D^{-\beta}$. One can easily show that the conditions defining the situation for $\sigma_{\text{PB}} > \sigma_D$ are given by

$$\beta < \frac{2 \ln(\rho^*/\rho)}{\ln(d/D)}. \quad (3)$$

In a system such as porous gold [10], $d = 15$ nm, $D \sim 1000$ nm, $\rho^*/\rho = 0.3$, we estimate that for $\beta < 0.57$ the porous system will display a larger yield stress than a solid 1 μm diameter gold pillar.

2. Sample-size effects: whiskers and pillars

The load–displacement behavior of gold whiskers and FIB-machined pillars is reproduced from the data of Brenner [13] and Greer et al. [3], respectively, in Fig. 3. In the case of the gold whisker the upper yield stress corresponds to about 0.02 of the shear modulus, G , and for the gold pillar the yield stress corresponds to about 0.027 G . Conventional polycrystalline gold has a yield stress of order 0.03 GPa or about 0.001 G . Using a first-principles calculation of the unstable stacking energy for gold slip along $\langle 10\bar{1} \rangle/\{111\}$ [15] we estimate that the theoretical shear strength, τ_{th} , for gold to be 0.07 G , so for the gold pillar the yield stress corresponds to about 0.4 of the theoretical shear strength.

The different load–displacement behaviors displayed in Fig. 3 are striking. The behavior displayed by the gold whisker is representative of behaviors for many face-

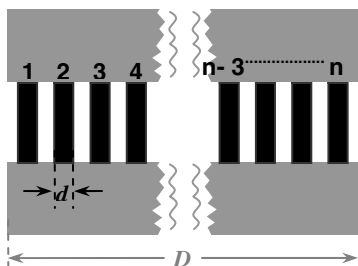


Fig. 2. Parallel bar array model composed of n uniformly spaced bars of diameter d and width D .

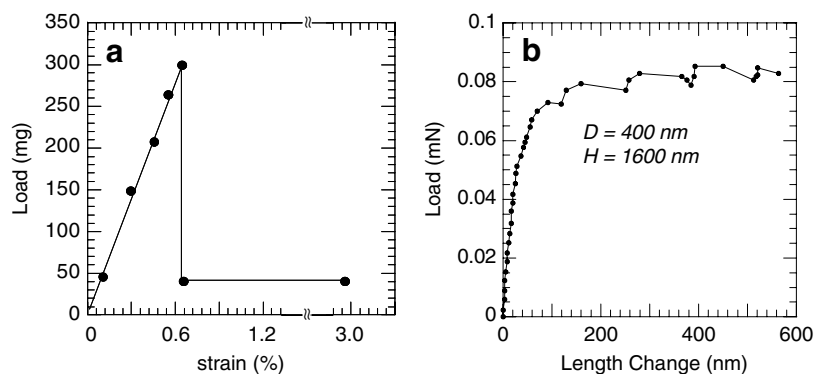


Fig. 3. (a) Load–strain behavior of a 400 μm long gold whisker of radius 1.3 μm . The maximum load of 300 mg corresponds to a stress level of 0.5 GPa. Data from Ref. [13]. (b) Load–displacement behavior of a 1600 nm high $\langle 001 \rangle$ gold pillar 400 nm in diameter. The maximum load corresponds to a flow stress of 0.55 GPa. Data from Ref. [3]. The Reuss average shear modulus of gold is 24 GPa. The shear modulus for $\langle 10\bar{1} \rangle / \{111\}$ slip is 18 GPa.

centered cubic (fcc) metal whiskers (Ag, Cu, etc.) except that in some instances even ductile fcc metals such as copper were observed to fracture at shear stress levels, $\tau/G \approx 0.02$, without any indication of irreversible deformation [13]. At strain values past the lower yield point deformation proceeds with no hardening via propagation of Lüders bands along the length of the whisker. The FIB-machined pillar displays quite different behavior in that the flow stress is maintained at values near or above the yield stress. This behavior has been referred to by Nix and co-workers as “dislocation starvation” [2]. The general notion is that owing to the small sample size, a nucleated dislocation has no opportunity to multiply (i.e., interact with other dislocations) as in ordinary plasticity displayed by conventional polycrystalline materials. The implication is that plastic flow, i.e., past yield, must involve continued nucleation events similar in nature to that responsible for the initial yielding phenomena.

A size-scale effect is a change in material properties due to a change in either the dimensions of features internal to the microstructure (internal length scale) or in the macroscopic dimensions of the sample (sample-size effect). Length-scale effects are readily observed in metals, e.g., the improvement of yield strength of metallic alloys through refinement of the grain size as described by the Hall–Petch relation, where the yield strength is proportional to the inverse square root of the average grain diameter, $\tau_{\text{yield}} \propto 1/\sqrt{d}$. The behavior is observed for grain sizes ranging from millimeters to about 10 nm; however, there are no unique routes or mechanisms for obtaining this scaling relation or ones of a similar nature (i.e., $\tau_{\text{yield}} \propto 1/d$).

3. Three size scales in crystal plasticity

Classic constitutive relations for plastic materials assume that mechanical properties are independent of sample size, in spite of results of experiments and simulations indicating that crystals exhibit size effects at the sub-micrometer scale. Dislocation theory and single-crystal plasticity, which developed throughout the past century, delivered the proper framework for understanding plastic-

ity in most metals for the macroscale and larger size scales (greater than several micrometers). The existence of many types of dislocations and the corresponding variety of nucleation, motion and mutual interaction mechanisms have been thoroughly investigated.

At size scales below a few micrometers, new phenomena appear as illustrated by the load–displacement behavior of whiskers and pillars. Currently the operative mechanisms for irreversible deformation at these size scales are not well understood and it is this regime that has been the focus of this discussion.

At size scales of the order of 10 nm and below a new regime of behavior emerges. Here, curvature and surface stress effects become important. For example, consider a 10 nm diameter gold cylinder with isotropic surface excess free energy, γ , and surface stress, f . The Laplace pressure in a cylinder of radius r is given by $P = f/r$ [16], and taking $f = 2.8 \text{ N/m}$ (a representative value for gold [16]), we obtain 0.28 GPa. We can expect that this large pressure would have significant effects on both elastic and plastic properties. For example one would expect to observe increases in the elastic constants and asymmetries in the plastic behavior of such cylinders tested in tension and compression. Additionally, new irreversible deformation modes involving structural transitions would set in at these small size scales. A number of researchers have observed these phenomena [17–21]. Using atomic force microscopy, Marszalek et al. [22], examined the behavior of 1.1 nm diameter gold wires in tension and compression. They found that these nanowires elongated in quantized steps of 0.176 nm and shortened spontaneously in steps of 0.152 nm during which the wires underwent a series of fcc \rightarrow hexagonal close-packed (hcp) \rightarrow fcc structural transitions. These transitions apparently correspond to rigid block-on-block sliding of atomic planes.

4. Surface effects in crystal plasticity

There has been a great deal written concerning surface effects in crystal plasticity relating to dislocation nucleation and the existence of soft or hard surface layers (see, e.g.,

Ref. [23]). In this regard, it is interesting to consider the issue of whether a clean surface presents a barrier to dislocation egress. Specifically this question was considered by Nabarro [23,24], who examined whether or not the energy per unit length of a dislocation (with a Burgers vector component normal to the free surface) can account for the energy per unit length associated with surface step creation (i.e., the self-energy of the step). He examined this issue for many fcc metals and some hcp metals and found that except for the case of lead the dislocation energy is more than enough to account for the surface step. The situation for isolated partials was different. Here, he found that the step energy always exceeded that of the dislocation, so presumably for this case the surface could act as a source of crystal “hardening”.

Here is an interesting contribution to this issue based on the now well-accepted idea that surface steps interact with one another elastically [25]. Fig. 4 shows schematically a cylinder that has already undergone some dislocation-mediated plastic flow and slip band formation. A dislocation is about to nucleate from the surface source at P and another is about to exit at P' . The incipient step at both a nucleation site P and an egress site P' will interact with existing steps on the surface so that the step energy is now composed of a self-energy term and an interaction term that depends on step height, step separations and total number of steps. (We note that this interaction was unknown at the time that Nabarro considered this problem.) Each step dipole has a moment of fh and a dilatation $h\omega$, where h is the step height. The elastic interaction energy among a step, j , and N steps in the train or deformation band is given by

$$E_{\text{int}} = C \sum_{i=1, i \neq j}^N (n_i h_i)^2 (\omega^2 + f^2) d_{ij}^{-2}$$

where $C = (1 - \nu)/\pi G$, ν is Poisson's ratio, G is the shear modulus, $n_k h_k$ is the step height (i.e., h is the elementary step height) and d_{ij} is the distance between the i th and j th step [25]. We have evaluated the magnitude of this interaction term for a generic fcc metal and find that for a train of steps containing 100 dislocations (corresponding to a displacement of the order of 10 nm) the interaction term is sig-

nificantly larger than the self-energy of the emerging dislocation. If we add the self-energy term of the step which is already near in value to that of the dislocation, we find that this interaction among steps can in principle serve as a source of hardening by making the process of creating additional steps more energetically expensive. Only atomic-scale calculations can provide realistic numbers for this as the continuum formulation can be expected to break down for high step densities.

5. Indentation size effect

Continuum-based strain gradient plasticity theories have been used to explain size effects in indentation experiments. Here, one can observe a hardness increase by factors of 3 as indentation contact radii decrease from 10^4 to 10^2 nm. This indentation size effect (ISE) phenomenon has been explained using strain gradient plasticity models that incorporate the concept of geometrically necessary dislocations. Theories such as the phenomenological model by Fleck and Hutchinson [26] or the microstructurally based model by Nix and Gao [27] appeared at one time to model effectively these size effects; however, nanoindentation experiments on tungsten, aluminum, gold and Fe-3 wt.% Si single crystals by Gerberich et al. [28] demonstrated that the underlying assumptions of these models do not hold for nanoindentation (<100 nm). They measured average plastic strains, and plastic zone sizes, from which they estimated strain gradients, showing that hardness decreased with increasing depth, irrespective of the sign or magnitude of the strain gradient. As such, strain gradient theory appears insufficient to explain the ISE. Clearly, the size effects reported by Nix, Volkert and co-workers for the homogenous compression of FIB-machined and electro-deposited cylinders cannot be associated with strain gradients.

6. Extreme value statistics and yield behavior

Over a period of time, between about 1985 and 1995, statistical physicists became interested in the fracture of “damaged” solids and considerable progress was made (see, e.g., Ref. [9]). We believe that yielding of (nearly) perfect crystals is a problem analogous to that of brittle fracture of glass rods for which it is generally accepted that surface flaws and weakest link statistics (Weibull and modified Gumbel forms) describe the phenomenon. If surface sites control nucleation of dislocations in FIB-machined pillars then the likelihood of nucleation at a particular value of shear stress will depend on the magnitude of the largest stress concentrator at the surface.

For fracture of randomly defective solids the prediction from statistical models yields forms for the fracture stress such as $\sigma_{\text{fracture}} \propto L^b$ or $\sigma_{\text{fracture}} \propto (\ln L)^{-y}$, where b and y are positive and the appropriate forms depend on the nature of the defect distribution. Fig. 5 shows data for the flow stress of Ni3Al–Ti [2] and gold pillars [3]. The

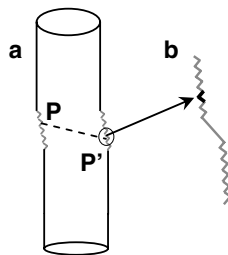


Fig. 4. (a) Cylinder deformed such that a slip band has developed. (b) Magnified view of step structure. The arrow points to an incipient step (black) associated with the egress of the dislocation at P' . An analogous situation is occurring at P related to the nucleation of a dislocation and incipient step formation.

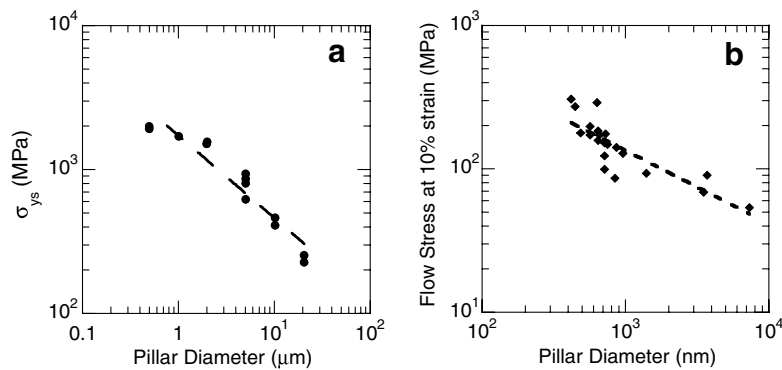


Fig. 5. Data for pillar compression yield strength versus diameter demonstrating power-law behavior as would be expected based on Weibull extreme value statistics. (a) Ni₃Al–Ti; the dotted line is a power-law fit $\sigma_{\text{yield}} \propto d^{-\beta}$, with $\beta = 0.57$. Data re-plotted from Ref. [2]. (b) Data for single-crystal gold columns. The dotted line is a power-law fit $\sigma_{\text{yield}} \propto d^{-\beta}$, with $\beta = 0.51$. Data re-plotted from Ref. [3].

exponents of the power-law fits are very close in numerical value which from an extreme value statistical view would indicate that the nature of the (surface) defects controlling dislocation nucleation is similar for these FIB-machined pillars.

7. Concluding remarks

We have introduced some new ideas related to deformation of materials at small length scales that are consistent with experimental results. The appropriateness of extreme value statistics to yield behavior can in principle be tested in the case of FIB-machined pillars by examining the nature of the strength fluctuations at fixed pillar diameter. Our discussion of surface effects and hardening behavior is most adequately addressed by atomic-scale simulation using techniques such as molecular dynamics. Experimentally, the surface step-induced hardening that we discuss may be difficult to decouple from conventional single-crystal kinematic hardening. However, we suggest that surface modification involving adsorption of foreign components may be a means of exploring surface step-induced hardening as this will undoubtedly alter the magnitude of the elastic dipoles. In principle, such adsorption could either lead to a further enhancement in hardening or even softening depending on how the surface stress is altered. Separate experiments using techniques such as wafer curvature could be used to measure changes in surface stress on adsorption and so make predictions of how a particular impurity may affect hardening or softening behavior.

Acknowledgement

The authors gratefully acknowledge support of this work and the Nanomechanics cluster by the Fulton School of Engineering at ASU.

References

- [1] Doremus RH, Roberts BW, Turnbull D, editors. Growth and perfection of crystals. New York: John Wiley; 1958.
- [2] Uchic MD, Dimiduk DM, Florando JN, Nix WD. Science 2004;305:986.
- [3] Greer JR, Oliver WC, Nix WD. Acta Mater 2005;53:1821.
- [4] Greer JR, Nix WD. Appl Phys A 2005;80:1625.
- [5] Volkert CA, Lilleodden ET. Philos Mag, in press.
- [6] Volkert CA, Lilleodden ET, Kramer D, Weissmuller J. submitted for publication.
- [7] Hirth JP. In: Relation between structure and strength in metals and alloys. London: HMSO; 1963. p. 218.
- [8] Nabarro FRN. Adv Phys 1952;1:269.
- [9] Duxbury PM. In: Herrmann HJ, Roux S, editors. Statistical models for the fracture of disordered media. Amsterdam: North Holland; 1990. p. 189.
- [10] Li R, Sieradzki K. Phys Rev Lett 1992;68:1168.
- [11] Webb WW. J Appl Phys 1965;36:214.
- [12] Weertman J. Phys Rev 1957;107:1259.
- [13] Brenner SS. J Appl Phys 1956;27:1484.
- [14] Gibson LJ, Ashby MF. Cellular solids. New York: Pergamon; 1988. p. 129.
- [15] Mehl MJ, Papaconstantopoulos DA, Kiousis N, Herbranson H. Phys Rev B 2000;61:4894.
- [16] Cammarata RC, Sieradzki K. Annu Rev Mater Sci 1994;24:215.
- [17] Agrait N, Rubio G, Viera S. Phys Rev Lett 1995;74:3995.
- [18] Coura PZ, Legoas SB, Moreria AS, Sato F, Rodrigues V, Dantas SO, et al. Nano Lett 2004;4:1187.
- [19] Gall K, Diao J, Dunn ML. Nano Lett 2004;4:2431.
- [20] Rubio G, Agrait N, Viera S. Phys Rev Lett 1996;76:2302.
- [21] Rubio-Bollinger G, Bahn SR, Agrait N, Jacobsen KW, Viera S. Phys Rev Lett 2001;87:026101-1.
- [22] Marszalek PE, Greenleaf WJ, Li H, Obserhauser AF, Fernandez JM. PNAS 2000;97:6282.
- [23] Latanision RM, Fourie JT, editors. Surface effects in crystal plasticity. The Netherlands: Noordhoff; 1977.
- [24] Nabarro FRN. In: Latanision RM, Fourie JT, editors. Surface effects in crystal plasticity. Noordhoff; 1977. p. 49.
- [25] Kukta RV, Peralta A, Kouris D. Phys Rev Lett 2002;88:186102-1.
- [26] Fleck NA, Hutchinson JW. J Mech Phys Solids 1993;41:1825.
- [27] Nix WD, Gao H. J Mech Phys Solids 1998;46:411.
- [28] Gerberich WW, Tymiak NI, Grunian JC, Horstmeier MF, Baskes MI. J Appl Mech 2002;69:433.